ESTIMATION OF DIFFERENTIAL INTER-SYSTEM BIASES BETWEEN THE OVERLAPPING FREQUENCIES OF GPS, GALILEO, BEIDOU AND QZSS

Dennis Odijk[1] **and Peter J.G. Teunissen**[1,2]

[1]*GNSS Research Centre, Department of Spatial Sciences, Curtin University, Perth WA 6845, Australia*
[2]*Department of Geosciences and Remote Sensing, Delft University of Technology, Delft, The Netherlands*

ABSTRACT

Multiple global and regional navigation satellite systems are currently being developed. In addition to the already available GPS and GLONASS constellations, Galileo and BeiDou satellites have been launched, as well as one QZSS satellite and other regional satellites. At the same time GPS and GLONASS are being modernized. High-precision positioning applications that rely on carrier-phase ambiguity resolution are likely to benefit from the many more satellites and frequencies that become available. Advantage can be taken from the fact some of the frequency bands are overlapping between the different constellations, since these signals may be differenced relative to one common reference satellite, instead of selecting a reference satellite per constellation. However, in case of relative positioning based on multi-GNSS receivers of different manufacturers, it is necessary to correct the data for nonzero differential inter-system biases (DISBs). In this contribution we present values for the DISBs, for the identical frequencies of GPS and Galileo, Galileo and BeiDou, as well as GPS and QZSS, based on multi-GNSS data provided in the context of the Multi-GNSS Experiment (MGEX).

Key words: Multi-GNSS; GPS; Galileo; BeiDou; QZSS; Differential Inter-System Biases.

1. INTRODUCTION

High-precision (centimeter level) carrier-phase integer-ambiguity-resolution-based positioning is expected to benefit significantly from the modernization of the U.S. Global Positioning System (GPS), together with the development of new global and regional navigation satellite systems. Many more satellites will be in view, transmitting data at many more frequencies than currently is the case with (dual-frequency) GPS only.

At present, of the new constellations the following satellites have been launched and are transmitting navigation signals: 4 European Galileo In-Orbit Validation (IOV) satellites, 14 Chinese BeiDou satellites and 1 Japanese Quasi-Zenith Satellite System (QZSS) satellite, where all satellites of BeiDou and QZSS can be tracked in the Asia-Pacific region. In addition, as part of the modernization of GPS there are currently 4 Block-IIF satellites transmitting the new L5 signal. Also the Russian GLONASS has been revitalized and is fully operational at the moment. However, GLONASS is left outside the scope of the present contribution, since it employs the Frequency Division Multiple Access (FDMA) technique, which is known to raise issues for carrier-phase ambiguity resolution [1]. These issues do not occur for the other systems, which are all based on the Code Division Multiple Access (CDMA) technique.

The availability of the new satellites requires a revision of the current differencing algorithms which were originally developed for GPS. Although these algorithms could be applied to the new constellations as well, there are better ways for combining the multi-GNSS observations. One of the aspects of such combination is to make advantage of the identical frequencies between the different constellations. Table 1 gives an overview of the frequencies and wavelengths of the signals of the GPS, Galileo, BeiDou and QZSS constellations. The identical frequencies between the constellations then follow as: (i) GPS L1, Galileo E1 and QZSS L1, (ii) Galileo E6 and QZSS LEX, (iii) GPS L2 and QZSS L2, (iv) Galileo E5b and BeiDou B2, and (v) GPS L5, Galileo E5a and QZSS L5. Because the Galileo E6 frequency is not tracked by the receivers in this study (it is encrypted for commercial purposes), the combination of E6 with the LEX signal is left outside the scope of this paper.

For the above mentioned identical frequencies the possibility to difference the observations of both constellations with respect to a reference satellite of one of them is investigated (instead of differencing the observations for each constellation separately). Earlier research based on GPS data combined with data of the two Galileo In-Orbit Validation Element (GIOVE) satellites (retired in 2012) demonstrated that Differential Inter-System Biases (DISBs) are present when phase (and also code) observations of GIOVE at the E1 and E5a frequencies are differenced with respect to the data of a GPS satellite at the L1 and L5 frequencies, respectively [2]. However, these DISBs were only present for baselines formed by pairs of multi-GNSS receivers of *different* manufacturers; for pairs of receivers of the same manufacturer they could be neglected. Furthermore, the DISBs turned out to be so stable in time that they could be calibrated. These results are confirmed by [3] and [4], who computed DISBs based on GPS data together with data of the Galileo-IOV satellites, for certain combinations of mixed receivers. By means of a-priori correcting the phase and code data of one of the constellations, just one common reference satellite is sufficient for both constellations, resulting in a stronger combined model for relative positioning.

In this contribution we experimentally determine the DISBs for phase and code, not only between GPS and the Galileo-IOV data (i.e. L1-E1 and L5-E5a), but also between Galileo and BeiDou (E5b-B2), as well as between GPS/Galileo and QZSS, with QZSS transmitting on the three GPS frequency bands. The analysis is based on zero and short baselines formed by multi-GNSS receivers of several manufacturers, which comprise Trimble, Septentrio, Javad, Leica and Novatel. Zero and short (less than 100 meter) baselines are advantageous for the estimation of the DISBs, since the differential atmospheric errors are completely canceled out (zero baselines), or, reduce to an insignificant level (short baselines). In addition, for zero baselines multipath effects are largely eliminated. These zero and short baseline data sets are collected by multi-GNSS receivers that are part of the worldwide Multi-GNSS EXperiment (MGEX) network [6].

2. ESTIMATION OF DIFFERENTIAL INTER-SYSTEM BIASES

Traditionally, real-time kinematic (RTK) applications, i.e. positioning requiring centimeter level accuracy, are based on first forming between-receiver *single-differenced* (SD) phase and code observation equations, eliminating satellite-dependent biases. Assume a rover receiver with respect to a reference receiver, then the following SD observation equations can be set up, for satellite s and frequency j, for a multi-GNSS receiver tracking measurements of *two constellations*, first for the first constellation, referred to as constellation A, see e.g. [7]:

$$\begin{array}{lclll} E(\phi_j^{1_A}) & = & \rho^{1_A} & +\delta t_j^A & \\ E(\phi_j^s) & = & \rho^s & +\delta t_j^A & +\lambda_j a_j^{1_A s} \\ E(p_j^{1_A}) & = & \rho^{1_A} & +dt_j^A & \\ E(p_j^s) & = & \rho^s & +dt_j^A & \end{array} \quad (1)$$

for $j = 1, \ldots, f_A$ and $s = 2_A, \ldots, m_A$. The expectation operator is denoted as $E(\cdot)$. Furthermore, ϕ_j^s and p_j^s denote the SD observables for phase and code, respectively; ρ^s denotes the SD receiver-satellite range; δt_j^A and dt_j^A the SD receiver clock parameters for phase and code, respectively; and $a_j^{1_A s}$ denotes the *double-differenced* (DD) ambiguity parameter (in cycle), which is defined as the difference of a SD ambiguity with respect to the SD ambiguity of another satellite, referred to as *pivot* satellite, i.e. $a_j^{1_A s} = a_j^s - a_j^{1_A}$, and this ambiguity is an integer parameter. Thus, despite the observations being single differenced, we may parameterize the ambiguities as double differences. As a consequence of this, the interpretation of phase and code receiver clocks, as well as ambiguities reads as follows:

$$\begin{array}{lcl} \delta t_j^A & = & dt + \lambda_j(\delta_j^A + a_j^{1_A}) \\ dt_j^A & = & dt + d_j^A \end{array} \quad (2)$$

with dt the SD receiver clock (in meter), and δ_j^A (in cycle) as well as d_j^A (in meter) the SD receiver hardware delays for phase and code. Note that the SD ambiguity of the pivot satellite, i.e. $a_j^{1_A}$ gets lumped to the receiver clock for phase. For the second constellation, referred to as B, we can set up similar SD observation equations:

$$\begin{array}{lclll} E(\phi_l^{1_B}) & = & \rho^{1_B} & +\delta t_l^B & \\ E(\phi_l^q) & = & \rho^q & +\delta t_l^B & +\lambda_l a_l^{1_B q} \\ E(p_l^{1_B}) & = & \rho^{1_B} & +dt_l^B & \\ E(p_l^q) & = & \rho^q & +dt_l^B & \end{array} \quad (3)$$

for $l = 1, \ldots, f_B$ and $q = 2_B, \ldots, m_B$. It is furthermore assumed that the differential atmospheric delays can be neglected (zero/short baselines), such that there are no unknown atmospheric parameters to be estimated.

The (biased) receiver hardware delays of both constellations, i.e. δ_j^A and δ_l^B for phase, and d_j^A and d_l^B for code, are assumed to be different between the two constellations, despite the signals are tracked inside one receiver, even if the frequencies are identical [8]. For both GNSSs also different pivot satellites are used, as to define the double-differenced (DD) ambiguities. Instead of solving the SD observation equations, we may also form DD observation equations by taking the difference of a SD observation with the SD of the pivot satellite, eliminating the receiver hardware biases, for constellation A:

$$\begin{array}{lcl} E(\phi_j^{1_A s}) = E(\phi_j^s - \phi_j^{1_A}) & = & \rho^{1_A s} + \lambda_j a_j^{1_A s} \\ E(p_j^{1_A s}) = E(p_j^s - p_j^{1_A}) & = & \rho^{1_A s} \end{array} \quad (4)$$

for $s = 2_A, \ldots, m_A$. For constellation B similar DD observation equations can be set up.

For frequencies that are *identical* between constellations A and B, we can also form double differences of one constellation with respect to the pivot satellite of the other constellation [9]. Suppose we take the pivot satellite of constellation A, then the observations at the identical frequencies of constellation B, denoted using subscript o, can be differenced with respect to this pivot satellite, such that their DD observation equations become:

$$\begin{array}{lclll} E(\phi_o^{1_A 1_B}) & = & \rho^{1_A 1_B} & +\lambda_o \delta_o^{AB} & \\ E(\phi_o^{1_A q}) & = & \rho^{1_A q} & +\lambda_o \delta_o^{AB} & +\lambda_o a_o^{1_B q} \\ E(p_o^{1_A 1_B}) & = & \rho^{1_A 1_B} & +d_o^{AB} & \\ E(p_o^{1_A q}) & = & \rho^{1_A q} & +d_o^{AB} & \end{array} \quad (5)$$

for $q = 2_B, \ldots, m_B$. Note that we have one additional Galileo double-difference for phase and code (between the pivot satellites of both constellations), but also one additional parameter for both phase and code, and these are referred to as *Differential Inter-System Biases* (DISBs):

$$\begin{array}{lcl} \delta_o^{AB} & = & (\delta_o^B - \delta_o^A) + (a_o^{1_B} - a_o^{1_A}) \\ d_o^{AB} & = & d_o^B - d_o^A \end{array} \quad (6)$$

Table 1. Frequencies and wavelengths of GPS, Galileo, BeiDou and QZSS ([1]E6 can only be tracked under Galileo's commercial service; [2] The QZSS LEX (L-band EXperiment) signal is designed to enable high-accuracy positioning in real-time through transmission of precise correction messages [5]).

Frequency (MHz)	1575.42	1561.098	1278.75	1268.52	1227.60	1207.14	1191.795	1176.45
Wavelength (cm)	19.03	19.20	23.44	23.63	24.42	24.83	25.15	25.48
GPS (G)	L1				L2			L5
Galileo (E)	E1		E6[1]			E5b	E5	E5a
BeiDou (C)		B1		B3		B2		
QZSS (J)	L1		LEX[2]		L2			L5

Table 2. Overview of constellations tracked by the multi-GNSS receivers in the tests (Y = yes; N = no). CUT = Curtin University, Perth, Australia; USN = United States Naval Observatory, Washington DC, US; SIN = Nanyang Technological University, Singapore; UNB = University of New Brunswick, Fredericton, Canada; WTZ = BKG, Wetzell, Germany.

Station ID	Receiver type	G	E	C	J
CUT0	Trimble NetR9	Y	Y	Y	Y
CUT1	Septentrio PolaRx4	Y	Y	Y	N
CUT2	Trimble NetR9	Y	Y	Y	Y
CUT3	Javad TRE-G3TH	Y	Y	Y	Y
USN4	Septentrio PolaRx4	Y	Y	N	N
USN5	Novatel OEM6	Y	Y	N	N
SIN1	Trimble NetR9	Y	Y	Y	Y
SIN0	Javad TRE-G3TH	Y	Y	N	Y
UNB3	Trimble NetR9	Y	Y	Y	N
UNBD	Javad TRE-G2T	Y	Y	N	N
UNBS	Septentrio PolaRxS	Y	Y	Y	N
WTZ2	Leica GR25	Y	Y	N	N
WTZ3	Javad TRE-G3TH	Y	Y	N	N
WTZR	Leica GRX1200+GNSS	Y	Y	N	N

where the phase DISB parameter is biased by the integer ambiguity between the pivot satellites of both constellations.

Knowing the DISBs, we can correct the phase and code observation equations of constellation B to improve the strength of the short-baseline model and consequently ambiguity resolution and RTK positioning. Let us denote the phase and code ISB corrections as:

$$\begin{array}{rcl} E(\tilde{\delta}_o^{AB}) & = & \delta_o^B - \delta_o^A + z_o \\ E(\tilde{d}_o^{AB}) & = & d_o^B - d_o^A \end{array} \quad (7)$$

with $z_o \in$ Z, the (unknown) integer inter-system ambiguity for the data set from which the ISBs are estimated. This notation is used as to discriminate this ambiguity from the inter-system ambiguity present in the observations that are corrected. The ISB-corrected single-differenced phase and code observation equations of constellation B become:

$$\begin{array}{rcl} E(\tilde{\phi}_o^q) = E(\phi_o^q - \lambda_o \tilde{\delta}_o^{AB}) & = & \rho^q + \delta t_o^A + \lambda_o \tilde{a}_o^{1_A q} \\ E(\tilde{p}_o^q) = E(p_o^q - \tilde{d}_o^{AB}) & = & \rho^q + dt_o^A \end{array} \quad (8)$$

for $q = 1_B, \ldots, m_B$ and with the estimable integer ambiguity $\tilde{a}_o^{1_A q} = a_o^{1_A q} - z_o$. From this it can be seen that it is not needed to know the integer z_0, since it gets estimable lumped to another integer, $a_o^{1_A q}$. In practice, it may be handy to subtract the integer that is closest to $\tilde{\delta}_o^{AB}$, such that the phase ISB becomes a *fractional* correction. Due to the phase and code ISB corrections, the single differences of constellation B become parameterized into the (biased) receiver clocks of constellation A, that thus can be eliminated by double differencing with respect to the pivot satellite of constellation A:

$$\begin{array}{rcl} E(\tilde{\phi}_o^{1_A q}) = E(\tilde{\phi}_o^q - \phi_o^{1_A}) & = & \rho^{1_A q} + \lambda_o \tilde{a}_o^{1_A q} \\ E(\tilde{p}_o^{1_A q}) = E(\tilde{p}_o^q - p_o^{1_A}) & = & \rho^{1_A q} \end{array} \quad (9)$$

for $q = 1_B, \ldots, m_B$. Now both DD observables as well as the estimable integer ambiguity for constellation B are relative to the pivot satellite of constellation A.

3. SELECTION OF MULTI-GNSS DATA

Table 2 presents an overview of the multi-GNSS receivers used for the estimation of the DISBs. All receivers that are grouped together (separated by the horizontal lines) are co-located: they are either connected to one common antenna to form a zero baseline, or to their own antenna to form a short baseline. The receivers with identification CUT are owned by Curtin University, where CUT0 is collecting data as part of the IGS-MGEX network, which also holds for the other receivers in the table (i.e. USN, SIN, UNB and WTZ). The only non-zero baselines are UNB3-UNBD and UNB3-UNBS, which are both short baselines of less than 20 m, as well as WTZ2-WTZR, a short baseline of almost 70 m.

As can be seen from Table 2, the baselines are formed by multi-GNSS receivers of different manufacturers. Trimble, Septentrio and Javad receivers are most used in the zero and short baseline setups. Other receivers are from Leica and Novatel. Note that for the Septentrio, Javad and Leica two different receiver types are involved: the Septentrio PolaRx4 and PolaRxS, the Javad TRE-G3TH and TRE-G2T, and the Leica GRX1200+GNSS and GR25. Although all involved receivers track GPS and Galileo data, BeiDou data are only available for receivers in Australia (CUT) and Canada (UNB). Data of the single Japanese QZSS satellite are only tracked by the receivers in Australia (CUT) and Singapore (SIN).

4. RESULTS OF DISB ESTIMATION

For several days in 2013 we estimated DISBs between the identical frequencies of GPS, Galileo, BeiDou and QZSS, based on the zero and short baseline data for the receivers given in Table 2. For the computation of the satellite positions we used broadcast ephemeris for all constellations. In this section we will first present the results for the DISBs between GPS and Galileo (i.e. L1-E1 and L5-E5a), after that between Galileo and BeiDou (E5b-B2) and finally between GPS and QZSS (L1, L2 and L5 for both constellations), as well as Galileo and QZSS (E1-L1 and E5a-L5).

4.1. Estimated DISBs between GPS and Galileo

As can be seen from Table 2, all receivers track data of both GPS and Galileo, so for all baselines it is possible to estimate DISBs between the constellations. As example, Figures 1 and 2 show the DISBs estimated for short (20 m) baselines UNB3-UNBD (Trimble-Javad) and UNB3-UNBS (Trimble-Septentrio). In addition, Figures 3 and 4 depict the results for zero baseline WTZ2-WTZ3 (Leica-Javad) and short (70 m) baseline WTZ2-WTZR (Leica-Leica). Plotted are the estimated DISBs, including their standard deviation based on the assumption that they are constant in time. The figures show that the estimated DISBs are non-zero, except for the Leica-Leica baseline, but they are reasonably stable during the time span. The noisier behavior after 8:00h GPST in Figures 1 and 2 is due to the lower elevation of the satellites that are used for the estimation of the DISBs at that time. Also multipath may have some effect here. The gaps in the time-series are caused by absence of observations, since both GPS and Galileo satellites are not continuously in view (for GPS we only used data of the 4 Block-IIF satellites that transmit the L5 signal).

The estimated phase and code DISB values shown in Figures 1, 2, 3 and 4 are consistent with the values obtained for other days, as well as for receivers at other locations. Similar values were obtained in [3], where DISBs are computed for mixed-receiver baselines, though restricted to the L1-E1 combination. To summarize, Tables 3 and 4, as well as Tables 5 and 6, present consistent values for the phase and code DISBs for all combinations of receiver manufacturers as present in Table 2, based on the values we have 'observed' (estimated) from the different baseline setups. In the tables the fractional phase DISBs are presented as values between –0.50 cyc and +0.50 cyc. We remark that a fractional phase DISB of –0.50 cyc is equivalent to a value of +0.50 cyc, since we may add an arbitrary integer. Note from the tables that for both phase and code there are combinations of mixed receivers for which the DISBs can be ignored (e.g. Javad-Septentrio for L1-E1). In addition to these 'observed' values, Tables 3, 4, as well as Tables 5 and 6 also contain values for receiver combinations for which we did not have baseline data available and which could not be estimated. However, from the values estimated from the receiver combinations that are observed, it is possible to *predict or derive* the DISB values for other combinations.

Table 3. Observed and derived **(fractional) phase DISBs [cycle] for GPS L1 and Galileo E1**. *The phase DISB is presented as a fraction within the interval* $-0.5 \leq DISB \leq 0.5$ *cycle. The values in italics are not estimated from real data (observed), but derived values.*

	Javad	Leica	Novatel	Sept.	Trimble
Javad	0	0.50	*0*	0	0.21
Leica	-0.50	0	*-0.50*	*-0.50*	*-0.29*
Novatel	*0*	*0.50*	*0*	0	*-0.21*
Sept.	0	*0.50*	0	0	0.21
Trimble	-0.21	*0.29*	*0.21*	-0.21	0

Table 4. Observed and derived **code DISBs [meter] for GPS L1 and Galileo E1**. *The values in italics are not estimated from real data (observed), but derived values.*

	Javad	Leica	Novatel	Sept.	Trimble
Javad	0	17.0	*22.2*	0	-2.0
Leica	-17.0	0	*5.2*	*-17.0*	*-19.0*
Novatel	*-22.2*	*-5.2*	*0*	-22.2	*-24.2*
Sept.	0	*17.0*	22.2	0	-2.0
Trimble	2.0	*19.0*	*24.2*	2.0	0

To see this, assume we have receivers of four different manufacturers, denoted as a, b, c and d. For the DISBs of these receivers we can set up the following table (for in this case phase, but for code it goes along similar lines):

$$\begin{array}{c|cc} & c & d \\ \hline a & \delta_{ac} & \delta_{ad} \\ b & \delta_{bc} & \delta_{bd} \end{array} \tag{10}$$

Note that when taking the difference of two columns yields the same value for each row (also holds for differencing between rows). where $\delta_{ac} = \delta_c - \delta_a$, etc. The DISB of a receiver pair that has not been observed, can be predicted based on the following condition:

$$(\delta_{ac} - \delta_{ad}) - (\delta_{bc} - \delta_{bd}) = 0 \tag{11}$$

Table 5. Observed and derived **(fractional) phase DISBs [cycle] for GPS L5 and Galileo E5a**. *The phase DISB is presented as a fraction within the interval* $-0.5 \leq DISB \leq 0.5$ *cycle. The values in italics are not estimated from real data (observed), but derived values.*

	Javad	Leica	Novatel	Sept.	Trimble
Javad	0	0.50	*0.50*	0.50	-0.03
Leica	-0.50	0	*0*	*0*	*0.47*
Novatel	*-0.50*	*0*	0	0	*0.47*
Sept.	-0.50	*0*	0	0	0.47
Trimble	0.03	*-0.47*	*-0.47*	-0.47	0

Table 6. Observed and derived **code DISBs [meter] for GPS L5 and Galileo E5a**. *The values in italics are not estimated from real data (observed), but derived values.*

	Javad	Leica	Novatel	Sept.	Trimble
Javad	0	19.5	*24.4*	0	-6.0
Leica	-19.5	0	*4.9*	*-19.5*	*-25.5*
Novatel	*-24.4*	*-4.9*	*0*	-24.4	*-30.4*
Sept.	0	*19.5*	24.4	0	-6.0
Trimble	6.0	*25.5*	*30.4*	6.0	0

For example, for a = Novatel, b = Trimble, c = Novatel, d = Septentrio, the code DISB between Trimble and Novatel can be predicted as $\delta_{bc} = (\delta_{ac} - \delta_{ad}) + \delta_{bd}$ = 0 + 24.4 + 6.0 = 30.4. These 'predicted' values should of course be verified by means of real observations. For some receiver combinations for which we have predicted the DISBs, the predicted values can be confirmed by the observed values of others [3, 4].

4.2. Estimated DISBs between Galileo and BeiDou

Similar to the identical frequencies of GPS and Galileo, the DISBs can be estimated between the identical frequency of Galileo and BeiDou, i.e. E5b and B2. Figures 5 and 6 show the phase and code DISBs estimated for zero baselines CUT0-CUT1 and CUT0-CUT3, as well as the 20-m baseline UNB3-UNBS. Both baselines CUT0-CUT1 and UNB3-UNBS combine a Trimble with a Septentrio, where the type of Septentrio receiver is a PolaRx4 for CUT1 and a PolaRxS for UNBS. Baseline CUT0-CUT3 is a Trimble-Javad combination. Since we only have BeiDou data available based on receivers of three manufacturers, we are only able to present results for combinations of Javad, Septentrio and Trimble. The estimated DISBs are reasonable constant in time for CUT0-CUT3, see Fig. 5 (right), as well as for UNB3-UNBS, where the DISBs are estimated for time spans on two different days: 1 April 2013, see Fig. 6 (left), vs. 17 October 2013, see Fig. 6 (right), although it is suspected that multipath is biasing the results somewhat.

Table 7. Observed **(fractional) phase DISBs [cycle] for Galileo E5b and BeiDou B2**. *The phase DISB is presented as a fraction within the interval* $-0.5 \leq DISB \leq 0.5$ *cycle. The upper table presents the phase DISB values before the update of the Septentrio firmware (at CUT1); the lower table those after the update.*

	Javad	Sept.	Trimble
Javad	0	-0.48	0.09
Sept.	0.48	0	-0.43
Trimble	-0.09	0.43	0

	Javad	Sept.	Trimble
Javad	0	0.02	0.09
Sept.	-0.02	0	0.07
Trimble	-0.09	-0.07	0

Table 8. Observed **code DISBs [meter] for Galileo E5b and BeiDou B2**.

	Javad	Sept.	Trimble
Javad	0	0.3	-2.6
Sept.	-0.3	0	-2.9
Trimble	2.6	2.9	0

In Fig. 5 (left), which shows the estimated DISBs for zero baseline CUT0-CUT1 during the full day of 2 August 2013, the phase DISB shows a jump of –0.5 cyc at about 7:36h GPST. The DISBs of zero baseline CUT0-CUT3 however do not show such a jump at that time, see Fig. 5 (right). The cause for this jump can be explained as follows. At that point of time the firmware of the Septentrio receiver at CUT1 was updated, to account for a 0.5 cycle offset between the Geostationary and the other satellites of BeiDou [10], which resulted in a 0.5 cycle shift of the DISB between the Trimble and Septentrio receiver. While the Trimble and Javad receivers experience a similar cycle offset, their receiver firmware has not been updated so far. Also the firmware of the Septentrio receiver at UNBS in Canada has not been updated yet, as the estimated phase DISB is still (17 October 2013) at the 'old' level of 0.43 cyc, see Figure 6 (right).

4.3. Estimated DISBs between GPS/Galileo and QZSS

QZSS transmits its signals on all three GPS frequencies, which are identical to two Galileo frequencies. We will compute DISBs based on the (currently) four GPS Block-IIF satellites that transmit all three frequencies. Since QZSS transmits the new L2C signal, the GPS L2C will be used in the DISB computation. Concerning L1, de-

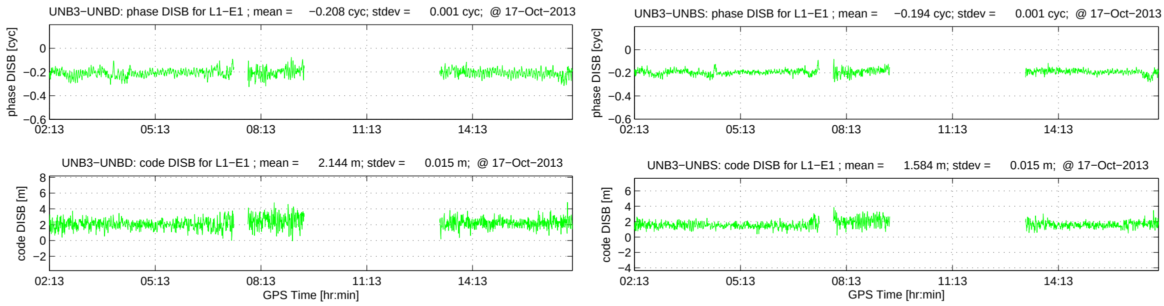

Figure 1. Estimated (fractional) phase DISBs (top) and code DISBs (bottom) between **GPS L1 and Galileo-IOV E1** *for short baseline between (left:) UNB3* **(Trimble)** *and UNBD* **(Javad)***, and (right:) UNB3* **(Trimble)** *and UNBS* **(Septentrio)***, during 17-Oct-13. The top row of the plots shows the fractional phase DISBs; the bottom row the code DISBs.*

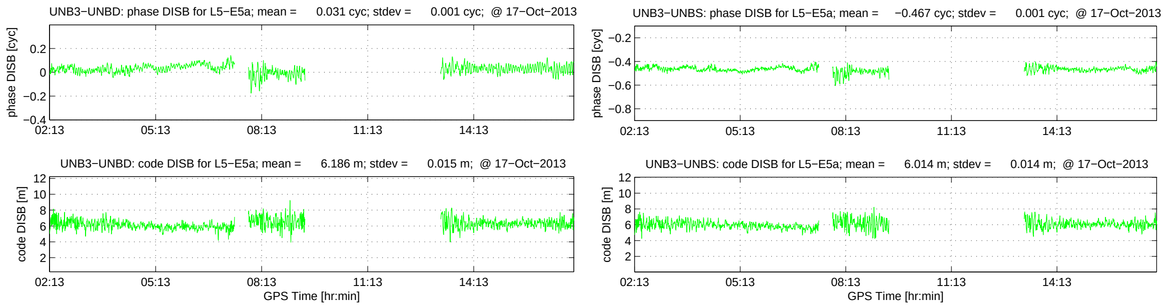

Figure 2. Estimated (fractional) phase DISBs (top) and code DISBs (bottom) between **GPS L5 and Galileo-IOV E5a** *for short baseline between (left:) UNB3* **(Trimble)** *and UNBD* **(Javad)***, and (right:) UNB3* **(Trimble)** *and UNBS* **(Septentrio)***, during 17-Oct-13. The top row of the plots shows the fractional phase DISBs; the bottom row the code DISBs.*

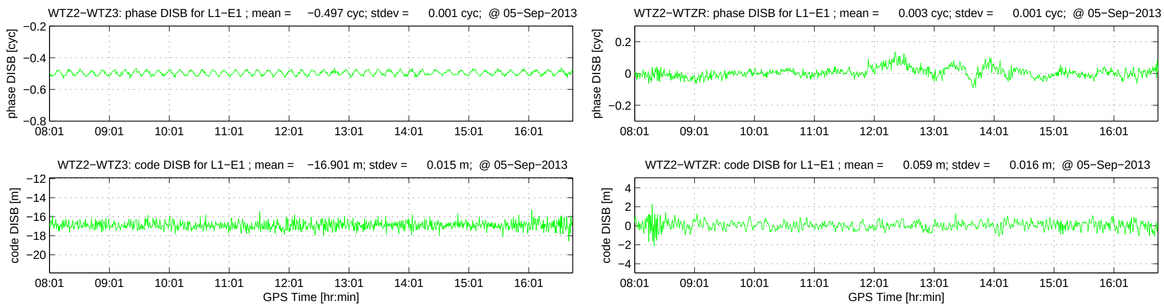

Figure 3. Estimated (fractional) phase DISBs (top) and code DISBs (bottom) between **GPS L1 and Galileo-IOV E1** *for zero baseline between (left:) WTZ2* **(Leica)** *and WTZ3* **(Javad)***, and short baseline between (right:) WTZ2* **(Leica)** *and WTZR* **(Leica)***, during 5-Sep-13. The top row of the plots shows the fractional phase DISBs; the bottom row the code DISBs.*

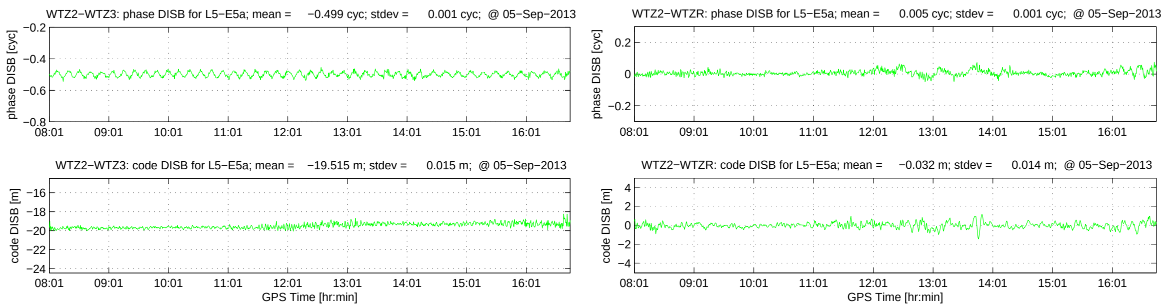

Figure 4. Estimated (fractional) phase DISBs (top) and code DISBs (bottom) between **GPS L5 and Galileo-IOV E5a** *for zero baseline between (left:) WTZ2* **(Leica)** *and WTZ3* **(Javad)***, and short baseline between (right:) WTZ2* **(Leica)** *and WTZR* **(Leica)***, during 5-Sep-2013. The top row of the plots shows the fractional phase DISBs; the bottom row the code DISBs.*

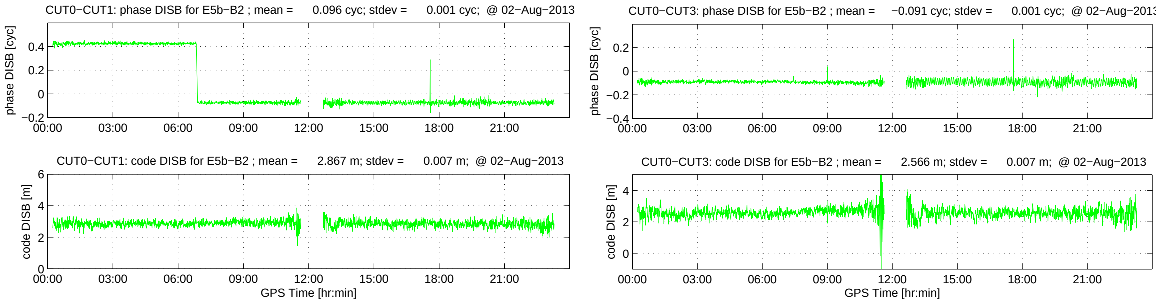

Figure 5. Estimated (fractional) phase DISBs (top) and code DISBs (bottom) between **Galileo-IOV E5b and BeiDou B2** *for zero baseline between (left:) CUT0* **(Trimble)** *and CUT1* **(Septentrio)***, and (right:) CUT0* **(Trimble)** *and CUT3* **(Javad)***, during 2-Aug-13. The top row of the plots shows the fractional phase DISBs; the bottom row the code DISBs. At 7:36 GPST the firmware of the Septentrio receiver at CUT1 was updated, to account for a 0.5 cycle offset between the Geostationary and the other satellites of BeiDou [10], resulting in a 0.5 cycle shift of the DISB between the Trimble and Septentrio receiver. Before the firmware update the mean phase DISB was 0.43 cyc; after the shift –0.07 cyc.*

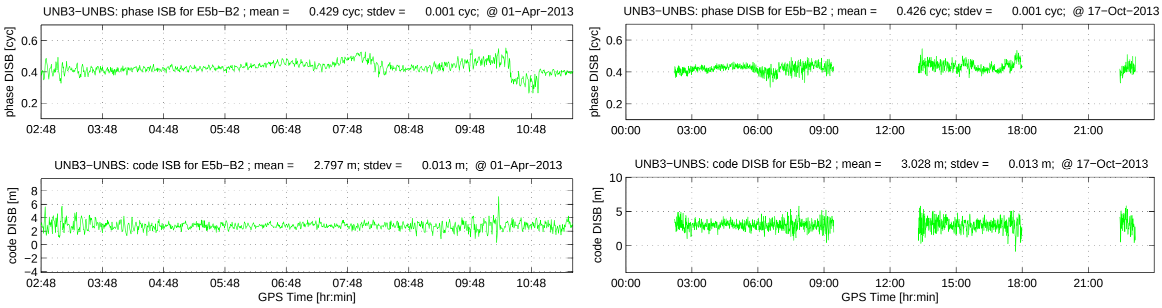

Figure 6. Estimated (fractional) phase DISBs (top) and code DISBs (bottom) between **Galileo-IOV E5b and BeiDou B2** *for short baseline between UNB3* **(Trimble)** *and UNBS* **(Septentrio)***, during 1-Apr-13 (left) and 17-Oct-13 (right). A gap in the time series means there are no Galileo and BeiDou satellites tracked at the same time. In this case the firmware of the Septentrio receiver has not yet been updated.*

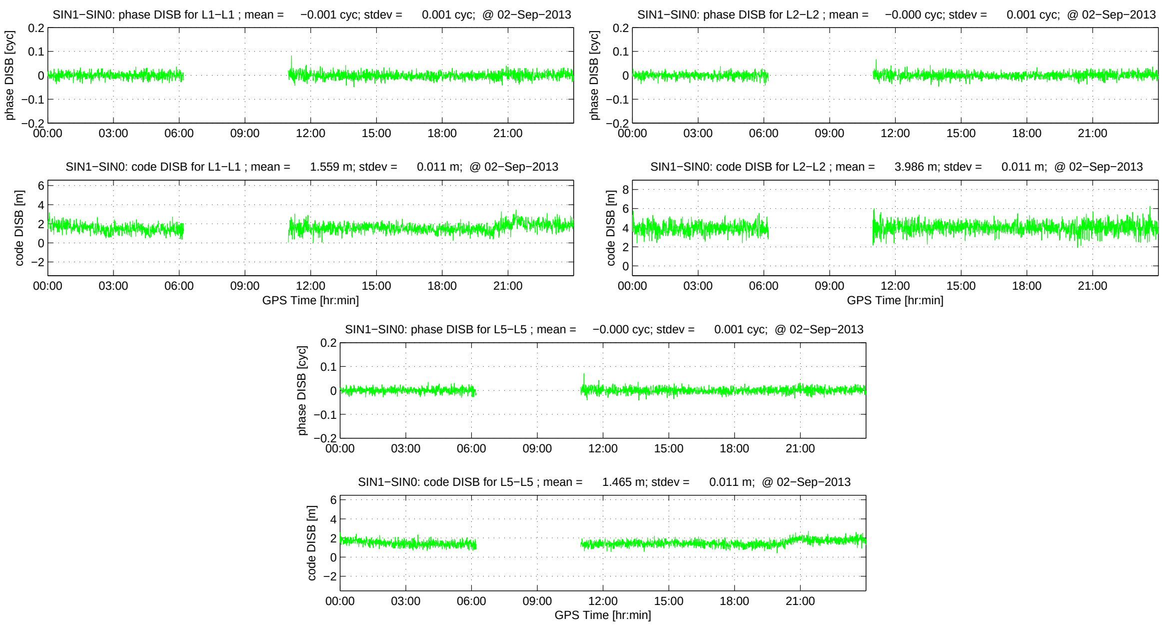

Figure 7. Estimated (fractional) phase DISBs (top) and code DISBs (bottom) between **GPS and QZSS** *for zero baseline between SIN1* **(Trimble)** *and SIN0* **(Javad)***, during 2-Sep-13, for* **L1C-L1C** *(top left),* **L2X-L2X** *(top right) and* **L5X-L5X** *(bottom). A gap in the time series means there are no GPS (Block-IIF) and QZSS satellites tracked at the same time.*

Table 9. Observed **DISBs for GPS and QZSS between Trimble and Javad**.

	phase DISB	code DISB
L1-L1	0 cyc	1.6 m
L2-L2	0 cyc	4.0 m
L5-L5	0 cyc	1.5 m

Table 10. Observed **DISBs for Galileo and QZSS between Trimble and Javad**.

	phase DISB	code DISB
E1-L1	0.21 cyc	-0.4 m
E5a-L5	-0.03 cyc	-4.5 m

pending on the receiver type different QZSS L1 observable types can be tracked on this frequency, such as L1C and L1X. Here we assume that both receivers forming the baseline track identical observable types (thus either L1C or L1X). Note from Table 2 that QZSS data are only received by the Trimble and Javad receivers, so we only present DISB results for this pair of mixed receivers.

Figure 7 shows the estimated DISBs between the three frequencies of GPS and QZSS obtained for zero baseline SIN1-SIN0, for 2 September 2013. As can be seen, the phase DISBs can be ignored, but this does not hold for the code DISBs. The mean values are given in Table 9. For the same baseline and the same day we also estimated the DISBs between the two identical frequencies of Galileo and QZSS, see Table 10 for their mean values. Note that these values are consistent with the values that can be predicted based on the estimated GPS-Galileo DISBs and the GPS-QZSS DISBs for the same receiver pair.

5. CONCLUSIONS

In this contribution we presented values for the DISBs based on multi-frequency phase and code data of current GPS, Galileo, BeiDou and QZSS, for different combinations of mixed multi-GNSS receiver pairs. Knowledge of these DISBs may strengthen the combined constellation model for ambiguity resolution based high-precision positioning, since when they are known, for the identical frequencies between constellations it is sufficient to take a pivot satellite from only one of the constellations to form double differences. We have demonstrated that for receiver pairs of the same manufacturer these DISBs can be ignored, whereas for many combinations of mixed receiver pairs the DISBs are present and significant, however very stable in time and may therefore be calibrated. However, we finally remark that the estimated/predicted DISB values as presented in this paper are based on limited data sets and should therefore be used with caution. More data processing is needed for verification.

ACKNOWLEDGMENTS

This work has been carried out in the context of the Positioning Program Project 1.01 ”New carrier phase processing strategies for achieving precise and reliable multi-satellite, multi-frequency GNSS/RNSS positioning in Australia” of the Cooperative Research Centre for Spatial Information (CRC-SI). The second author is the recipient of an Australian Research Council (ARC) Federation Fellowship (project number FF0883188). All this support is gratefully acknowledged.

REFERENCES

[1] F Takac. GNSS Solutions: What are the challenges associated with GLONASS (FDMA) ambiguity resolution and how are they addressed? *InsideGNSS*, March/April:24–28, 2009.

[2] D Odijk and P J G Teunissen. Characterization of between-receiver GPS-Galileo inter-system biases and their effect on mixed ambiguity resolution. *GPS Solutions*, 17(4):521–533, 2013.

[3] J Paziewski, P Wielgosz, K Stepniak, and R Sieradzki. Accounting for inter-system biases between Galileo and GPS (Poster). In *IAG Scientific Assembly, Potsdam, Germany, 1-6 September*, 2013.

[4] T Melgard, J Tegedor, K de Jong, D Lapucha, and G Lachapelle. Interchangeable integration of GPS and Galileo by using a common system clock in PPP. In *Proc. of ION GNSS+ 2013, Nashville, TN, 16-20 September*, 2013.

[5] S Zhang, S Choy, K Zhang, and S Wu. Performance evaluation of the Japanese Quasi-Zenith Satellite System (QZSS) LEX signal in Australia. In *Proc. of IGNSS 2013, Gold Coast, Australia, 16-18 July*, 2013.

[6] International GNSS Service (IGS). Multi-GNSS EXperiment (MGEX). `http://igs.org/mgex/`. Accessed October, 2013.

[7] B Hofmann-Wellenhof, H Lichtenegger, and E Wasle. *GNSS – Global Navigation Satellite Systems: GPS, GLONASS, Galileo & more*. Springer Wien New York, 2008.

[8] C Hegarty, E Powers, and B Fonville. Accounting for timing biases between GPS, modernized GPS, and Galileo signals. In *Proc. 36th Annual Precise Time and Time Interval (PTTI) Meeting, Washington, DC, 7-9 December*, pages 307–317, 2004.

[9] D Odijk, P J G Teunissen, and L Huisman. First results of mixed GPS+GIOVE single-frequency RTK in Australia. *Journal of Spatial Science*, 57(1):3–18, 2012.

[10] N Nadarajah, P J G Teunissen, and N Raziq. BeiDou inter-satellite-type bias evaluation and calibration for mixed receiver attitude determination. *Sensors*, 13:9435–9463, 2013.